

Increasing thermoelectric performance using coherent transport

O. Karlström¹, H. Linke¹, G. Karlström², A. Wacker¹

¹ *The Nanometer Structure Consortium (nmC@LU), Lund University, Box 118, SE-221 00, Sweden*

² *Division of Theoretical Chemistry, Department of Chemistry, Lund University, Box 124, SE-221 00, Sweden*

We show that coherent electron transport through zero-dimensional systems can be used to tailor the shape of the system's transmission function. This quantum-engineering approach can be used to enhance the performance of quantum dots or molecules in thermal-to-electric power conversion. Specifically, we show that electron interference in a two-level system can substantially improve the maximum thermoelectric power and the efficiency at maximum power by suppressing parasitic charge flow near the Fermi energy, and by reducing electronic heat conduction. We discuss possible realizations of this approach in molecular junctions or quantum dots.

PACS numbers: 72.20.Pa, 73.23.-b, 85.35.Ds

Thermoelectric devices are currently of high interest both for solid-state cooling and for increasing energy efficiency in converting heat into electric power. The efficiency of thermoelectric materials to convert a temperature gradient into electrical work is characterized by the figure of merit¹

$$ZT = \frac{S^2 \sigma T}{\kappa_{el} + \kappa_{ph}}, \quad (1)$$

with the temperature T , the Seebeck coefficient S , the electric conductance σ , as well as the electronic and phononic thermal conductance κ_{el} and κ_{ph} . Other important performance parameters are the power output $P = -(\mu_L - \mu_R)I$, the maximum power P_{max} at the optimal bias and level configuration, and the efficiency $\eta = P/J_Q$. Here, μ_L and μ_R are the chemical potentials of left and right bath, respectively, I is the particle current, and J_Q is the heat flux out of the warm bath.

Nanostructured materials are attractive candidates for efficient thermoelectrics, because they offer the opportunity to optimize S by using the energy-selectivity of charge carrier transport in low-dimensional systems² combined with the suppression of κ_{ph} by interface scattering.³ In such systems, I, S, σ, J_Q and κ_{el} can be directly evaluated from the electronic transmission function $\Sigma(E)$.⁴

In particular, zero-dimensional (0D) systems, such as quantum dots or molecules, that are weakly coupled to electron reservoirs, can be designed as ideal energy filters with an energy-dependent transmission function $\Sigma(E) \propto \delta(E - E_1)$, where E_1 is the position of the single level that contributes to transport. In this limit, and for $\kappa_{ph} = 0$, ZT diverges⁴ and the efficiency of thermoelectric power conversion approaches Carnot efficiency (η_C).^{5,6} Additionally, such ideal quantum dots reach the ideal Curzon-Ahlborn efficiency η_{CA} of about $\eta_C/2$ when E_1 is tuned to maximum power production P_{max} .⁷ However, the limit $\Sigma(E) \propto \delta(E - E_1)$ in 0D systems is not interesting for applications because the power output becomes exceedingly small, and even a small $\kappa_{ph} \neq 0$ leads to a low value of ZT . To increase the current and P_{max} in 0D systems one needs to broaden $\Sigma(E)$. This drastically reduces the efficiency at maximum power η_{maxP} , because

the Lorentzian-shaped $\Sigma(E)$ has a long low-energy tail that leads to a counter flow of cold charge carriers, contributing with opposite sign to S .⁸

Here, we show that coherent transport in 0D systems can be used to tailor $\Sigma(E)$ such that counter flow of cold charge carriers is effectively suppressed. In addition to its fundamental interest, this approach to quantum engineering is shown to substantially increase P_{max} , η_{maxP} and ZT compared to the ideal 0D systems addressed above. We discuss how this effect can be implemented in semiconductor quantum dots or in molecular junctions.

We consider a two-level system with both energy levels E_1, E_2 situated on one side of μ_L and μ_R , (Fig. 1(a)), such that the charging energy is of minor importance,⁹ and a spin degeneracy will not affect transport significantly. This setup is similar to the double-dot case¹⁰ addressed very recently in Ref. 11, where equal coupling strengths of the two levels were assumed. Related findings were presented in Ref. 12 where the thermoelectric properties of double quantum dots with couplings ranging from serial to parallel configurations were investigated, assuming equal energies of the two dots.

The coupling between lead and dot is parametrized as in Ref. 9, assuming equal coupling strengths to left and right leads. The two levels couple with different parity to the leads and their coupling strengths differ by a factor a^2 , $\Gamma_{L1} = \Gamma_{R1} = \Gamma$, $\Gamma_{L2} = \Gamma_{R2} = a^2\Gamma$. This difference in parity will turn out to be essential for the increased thermoelectric performance. For such couplings it can be shown that the Breit-Wigner formula provides results identical to the exact method of nonequilibrium Green's functions (NEGF)¹³

$$\Sigma(E) = \Gamma^2 \left| \frac{1}{E - E_1 + i\Gamma} - \frac{a^2}{E - E_2 + ia^2\Gamma} \right|^2, \quad (2)$$

where the two levels contribute with different sign due to the opposite parity. Vanishing transport at the Fermi energy $E_F \equiv 0$ corresponds to $E_2 = a^2 E_1$. A device operated close to such a level configuration would have the desired property that $\Sigma(0) \approx 0$ independently of Γ .

Fig. 2 shows that a large power factor $S^2\sigma$ is achieved for level positions over an energy range as large as several

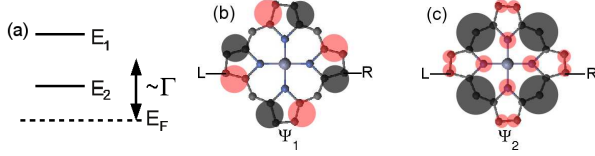


FIG. 1. (a) Level positions in the proposed two-level system. (b)-(c) Possible implementation using zinc porphine, sketching the wave functions of the two almost degenerate levels close to the Fermi energy, see also Ref. 14. The light/dark shaded regions indicate a positive/negative amplitude of the wave function Ψ , respectively. By replacing the hydrogen atoms at the positions L and R with, for example, sulfur the molecule can be contacted to leads so that the parity of the wave functions with respect to the leads differ for the two levels.

$k_B T$, ($k_B T \approx 0.26$ eV at $T = 300$ K). The transmission function at maximum power factor, which is marked by a cross in Fig. 2, is displayed in Fig. 3(a). The strong asymmetry in $\Sigma(E)$, with a sharp step facing E_F , is ideal for high power production.¹⁵ The decrease of $\Sigma(E)$ for large energies prevents the transmission of high-energy electrons, which reduces κ_{el} and results in an increased efficiency of the device.

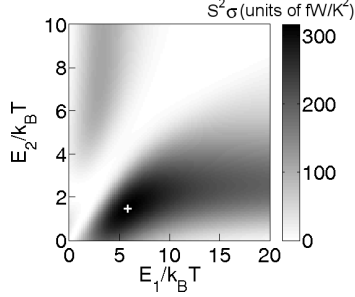


FIG. 2. The power factor for coherent transport through a quantum system with two levels and for $T = 300$ K, $\Gamma = 3k_B T_R$, and $a = 0.6$. Level positions are defined relative to E_F . The cross marks the maximum ($S^2\sigma = 316$ fW at $E_1 = 5.80k_B T$, $E_2 = 1.47k_B T$), and the transmission function is calculated at this level configuration in Fig. 3(a).

Fig. 3(b) displays $P_{\max}(\Gamma)$ for different values of the asymmetry parameter a , showing peak power values more than two times larger than the P_{\max} achievable in a single-level 0D system corresponding to $a = 0$. In the coherent case maximum power occurs for larger Γ , since the broadening of the levels is not such a severe problem. Fig. 3(c) shows the efficiency at maximum power $\eta_{\max P}$, which can be increased by over an order of magnitude, compared to the single level case, for large Γ . In the limit $\Gamma \rightarrow 0$ one observes that $\eta_{\max P} \rightarrow \eta_{CA} \approx 0.5\eta_C$.^{7,8} When Γ and a are small P_{\max} and $\eta_{\max P}$ are not substantially increased, since the effect of the second level is small when $k_B T \gg a^2 \Gamma$. As Γ is increased, the effect of the second level can be observed as an increase in P_{\max} and

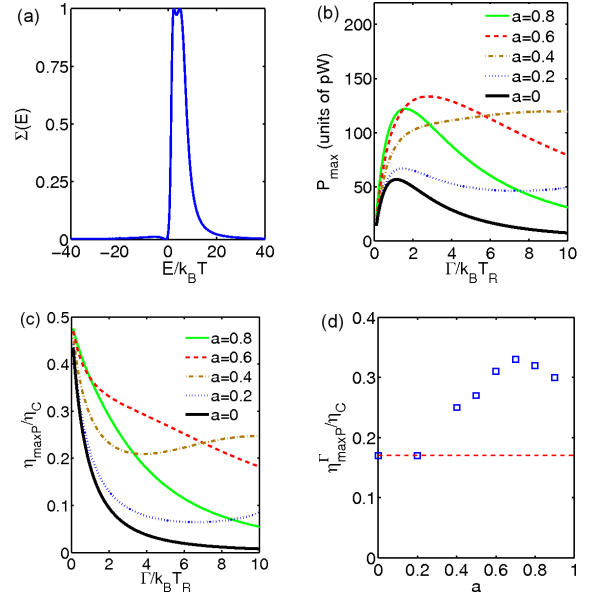


FIG. 3. (a) Transmission function at the level configuration corresponding to maximum power, see Fig. 2. (b) Maximum power production and (c) efficiency at maximum power $\eta_{\max P}$ in units of the Carnot efficiency η_C , as a function of Γ . (d) shows $\eta_{\max P}^\Gamma$ (defined as P_{\max} at the optimal choice of Γ , see text), with the dashed line marking the one-level result. In (b)-(d) the temperatures of the two leads are given by $T_L = 330$ K and $T_R = 300$ K.

$\eta_{\max P}$, which can result in a local maximum. Fig. 3(d) displays $\eta_{\max P}^\Gamma$, the efficiency at maximum power where the power production is optimized with respect to Γ as well as with respect to bias and level positions. We restrict ourselves to $\Gamma < 10k_B T_R$ where effects of the local maximum, present for small a , is not observed. For small a the presence of the second level is negligible, and the efficiency of a single level is approached. High efficiency is achieved close to $E_2 = a^2 E_1$. For $a \rightarrow 1$ the level configuration that yields P_{\max} does not coincide with $E_2 = a^2 E_1$ where transport is blocked (Eq. 2). Thus $\eta_{\max P}^\Gamma$ decreases for large a and the maximum is found around $a = 0.7$.

To facilitate the comparison with other work we present, in Fig. 4(a), the resulting figure of merit ZT_{el} , defined by $\kappa_{ph} = 0$ in Eq. (1). We see that even for the relatively large Γ resulting in maximum power, values as high as $ZT_{el} = 7$ can be reached. In part, this increase is due to a decrease in κ_{el} . It is worth noting that, for the realistic case of finite κ_{ph} , maximum ZT is expected near the conditions for P_{\max} (indicated by crosses in Figs. 2 and 4(a)), because a high power factor is needed in Eq. (1) to provide robustness against parasitic heat flow due to phonons.

Coherent transport through molecules has been discussed previously in Refs. 16 and 17, where the interference between levels positioned on different sides of E_F causes a dip in the transmission function at E_F . The

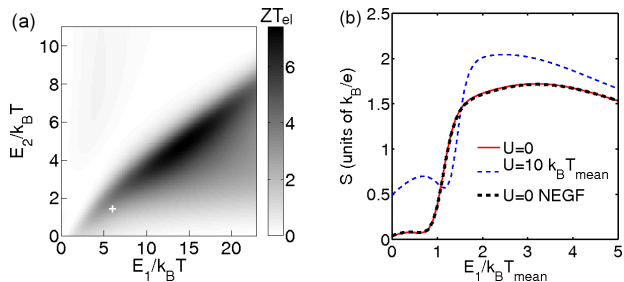


FIG. 4. (a) Thermoelectric figure of merit ZT_{el} for coherent transport as a function of level configuration for $T = 300$ K. The parameters $\Gamma = 3k_B T$, and $a = 0.6$ match the conditions for maximum power in Fig. 3(b). (b) The thermopower S calculated for $U = 0$ and $U = 10 k_B T_{\text{mean}}$, $\Gamma = k_B T_{\text{mean}}$, $a = 0.7$, and $\Delta T = 0.1 k_B T_{\text{mean}}$. The second level is positioned at $E_2 = k_B T_{\text{mean}}$.

corresponding reduction of charge flow near E_F can be used to increase the thermoelectric figure of merit, for example in molecules¹⁸ or quantum dots.¹⁹ However, the increased values of ZT_{el} obtained in these papers are a result of the decrease in κ_{el} . This results in low power output and in a high sensitivity to phonons¹⁸ because $ZT = ZT_{el}/(1 + \kappa_{ph}/\kappa_{el})$. Increased thermopower due to interference effects has also been discussed in the context of side-group induced Fano resonances.²⁰ While the thermoelectric performance was significantly improved, this approach is challenging because it requires very good control ($\sim 10^\circ$) of the tilting angle of the side group. Recently, efforts were made to determine which types of molecules exhibit Fano resonances,²¹ and investigate their thermoelectric performance.²²

We now discuss possible experimental implementations of coherent enhancement of thermoelectric efficiency: First, highly controllable 0D systems can be realized in the form of quantum dots defined in two-dimensional electron gases²³ or in nanowires.^{24,25} By electrostatically gating the quantum dot, its energy levels can be shifted so that mainly two states contribute to the transport. The relative position of the two levels with different parity can be controlled by applying a magnetic field,²⁵ in particular in quantum dot materials with a large g-factor such as InSb.²⁶ The use of two parallel coupled quantum dots allows for better control of the two levels, but coherence is decreased due to the spatial separation of the two dots.

The exquisite experimental control over semiconductor quantum dots thus makes them an excellent testbed for the fundamental study of the effects predicted here. However, the use of quantum dots in applications, for example in the form of nanocrystals embedded into bulk materials, is limited because it is very challenging to produce such dots with the high uniformity required to have equal energy levels in all dots.

An alternative system with inherently much better reproducibility are molecular junctions that fulfill the fol-

lowing requirements:

- i) The molecule must have two almost degenerate, conductive states with different parity. Such states can be found in molecules that are symmetric with respect to the leads, where the symmetry implies that the states must be symmetric and anti-symmetric.
- ii) The two states must be positioned within a few Γ of E_F (Fig. 2). The active states could be either LUMO-states which should be placed slightly above E_F , or HOMO-states which should be placed slightly below.

A possible candidate is zinc porphine (Fig. 1(b,c)). This molecule has two almost degenerate HOMO-levels with the desired parity.¹⁴ The relative position of the two levels can be changed by adding e.g. phenyl groups²⁷ or replacing all hydrogen atoms with e.g. chlorine or boron.¹⁴ To contact the molecule by gold electrodes one could replace two hydrogen atoms by sulfur (Fig. 1(b,c)). The leads can affect the molecular orbitals via charge transfer²⁸ and symmetry breaking. To include such effects, and calculate the transmission function of the system, one can use the method described in Ref. 29. A rough estimate of the coupling between lead and orbital i of the junction molecule is given by $\Gamma_i \approx 2\pi|\Psi_i|^2 C^2 N_0$, where Ψ_i is the value of the wave function at the sulfur, $C = 2$ eV is the matrix element between the gold and the sulfur atoms, and $N_0 = 0.07/\text{eV}$ is the gold density of states per atom per eV at E_F .³⁰ Assuming that the wave function is evenly distributed among the 20 carbon, 4 nitrogen, 1 zinc, and 2 sulfur atoms of zinc porphine gives $\Psi_i = (27)^{-1/2}$ and $\Gamma_i \approx 0.065$ eV $\approx 2.5 k_B T$ at $T = 300$ K. The actual values for Γ_i will vary between the different orbitals, but this estimate shows that the parameters are in a regime where coherent transport can be significantly more efficient than transport through a single level, (Fig. 3(b) and (c)).

We now turn to the effect of phonons on thermoelectric performance. Values around $\kappa_{ph} = 50$ pW/K have been experimentally determined for molecular wires,³ and $\kappa_{ph} = 10\ldots 100$ pW/K has been estimated for molecular junctions.³¹ For the parameters of Fig. 4(a) the latter results in impressive $ZT = 0.7\ldots 3$. These values are quite preliminary as the exact value of κ_{ph} depends on the junction molecule. However, it should be noted that experiments and theoretical calculations of the IR spectra of zinc porphine show that the majority of the vibrational transitions lie significantly above $k_B T$ at room temperature,³² suggesting a low κ_{ph} . Also any destructive effect of phonons on the coherence should not be a severe problem as the suggested operation point of the device is in the regime $\Gamma > k_B T$, i.e. the coherence time of the electron on the junction molecule is longer than the tunneling time, resulting in coherent transport. A more detailed study of the couplings between the low-energy vibrations and the electronic degrees of freedom is required.

So far we have not discussed the effects of electron-electron interaction. In the following we show that a finite charging energy U does not affect the results qual-

itatively, and may in fact result in an increased S . To include a finite U we use the second order von Neumann approach (2vN),³³ an equation of motion technique where co-tunneling as well as the coherence and charging energy between the levels are included. This approach calculates the current without directly calculating the transmission function $\Sigma(E)$, and S is calculated as the open-circuit voltage at a small but finite temperature gradient ΔT applied between the leads.

The 2vN-approach neglects certain tunneling events of higher order which results in less accurate results for lower temperatures. In Fig. 4(b) the thermopower is calculated for the temperatures $k_B T_L = k_B T_{\text{mean}} + \Delta T/2$ and $k_B T_R = k_B T_{\text{mean}} - \Delta T/2$. To investigate the importance of a finite U , E_2 has been placed slightly above E_F at $E_2 = k_B T_{\text{mean}}$. The thermopower is then calculated as a function of E_1 . To demonstrate that the 2vN method gives accurate results, and that the effect of the finite ΔT is negligible, the $U = 0$ results are compared to results obtained using NEGF. When $E_1 \approx 0$ the transport is dominated by this level, which results in a low thermopower in the case of $U = 0$. For a finite U part of the spectral density of E_1 is shifted to $E_1 + U$ due to

the small but finite occupation of level E_2 . This results in transport at increased energies, and consequently a higher thermopower. When E_1 is far away from E_F the difference between $U = 0$ and $U = 10 k_B T_{\text{mean}}$ decreases as the effect of the charging energy vanishes when the levels are empty.

In conclusion, we have shown how coherent transport can be used to tailor the shape of the system's transmission function, to combine a large thermoelectric power production with a high efficiency. Compared to transport through one-level systems, the maximum power production is more than doubled. At the same time efficiencies at maximum power up to $\eta_{\text{max}P} = 0.33$ are achieved for $\kappa_{ph} = 0$, comparable to those theoretically achievable in ideal (ballistic) one-dimensional devices where $\eta_{\text{max}P} = 0.36$ is expected.⁸ We also proposed a specific molecular junction for the implementation of this novel approach to thermoelectric engineering, and expect a ZT of the order of unity or above.

We thank Christian Bergenfeldt and Peter Samuelson for stimulating discussions. Financial support from the Swedish Research Council (VR), Energimyndigheten (Grant No. 32920-1), and nmC@LU is gratefully acknowledged.

-
- ¹ H. J. Goldsmid, *Thermoelectric Refrigeration* (Plenum Press, New York, 1964).
 - ² M. S. Dresselhaus, G. Chen, M. Y. Tang, R. G. Yang, H. Lee, D. Z. Wang, Z. F. Ren, J.-P. Fleurial, and P. Gogna, *Adv. Mater.* **19**, 1043 (2007).
 - ³ Z. Wang, J. A. Carter, A. Lagutchev, Y. K. Koh, N.-H. Seong, D. G. Cahill, and D. D. Dlott, *Science* **317**, 787 (2007).
 - ⁴ G. D. Mahan and J. O. Sofo, *Proc. Natl. Acad. Sci. U.S.A.* **93**, 7436 (1996).
 - ⁵ T. E. Humphrey, R. Newbury, R. P. Taylor, and H. Linke, *Phys. Rev. Lett.* **89**, 116801 (2002).
 - ⁶ C. V. den Broeck, *Adv. Chem. Phys.* **135**, 189 (2007).
 - ⁷ M. Esposito, K. Lindenberg, and C. V. den Broeck, *Europhys. Lett.* **85**, 60010 (2009).
 - ⁸ N. Nakpathomkun, H. Q. Xu, and H. Linke, *Phys. Rev. B* **82**, 235428 (2010).
 - ⁹ O. Karlström, J. N. Pedersen, P. Samuelsson, and A. Wacker, *Phys. Rev. B* **83**, 205412 (2011).
 - ¹⁰ P. Trocha and J. Barnaś, arXiv:1108.2422v1; G. Gómez-Silva, O. Ávalos-Ovando, M. L. Ladrón de Guevara and P. A. Orellana, arXiv:1108.4460v1.
 - ¹¹ Y. S. Liu, D. B. Zhang, X. F. Yang, and X. F. Yang, *Nanotechnology* **22**, 225201 (2011).
 - ¹² M. Wierzbicki and R. Swirkowicz, *Phys. Rev. B* **84**, 075410 (2011).
 - ¹³ This definition of Γ differs by a factor 2 from the one used in Ref. 8.
 - ¹⁴ H.-H. G. Tsai and M. C. Simpson, *Chemical Physics Letters* **353**, 111 (2002).
 - ¹⁵ T. E. Humphrey, M. F. O'Dwyer, and H. Linke, *J. Phys. D: Appl. Phys.* **38**, 2051 (2005).
 - ¹⁶ D. M. Cardamone, C. A. Stafford, and S. Mazumdar, *Nano Letters* **6**, 2422 (2006).
 - ¹⁷ S.-H. Ke, W. Yang, and H. U. Baranger, *Nano Letters* **8**, 3257 (2008).
 - ¹⁸ J. P. Bergfield and C. A. Stafford, *Nano Letters* **9**, 3072 (2009); J. P. Bergfield, M. A. Solis, and C. A. Stafford, *ACS Nano* **4**, 5314 (2010).
 - ¹⁹ T. Nakanishi and T. Kato, *Journal of the Physical Society of Japan* **76**, 034715 (2007).
 - ²⁰ C. M. Finch, V. M. García-Suárez, and C. J. Lambert, *Phys. Rev. B* **79**, 033405 (2009).
 - ²¹ T. Markussen, R. Stadler, and K. S. Thygesen, *Nano Letters* **10**, 4260 (2010); *Phys. Chem. Chem. Phys.* **13**, 14311 (2011).
 - ²² R. Stadler and T. Markussen, arXiv:1106.3661v1 (2011).
 - ²³ R. Scheibner, H. Buhmann, D. Reuter, M. N. Kiselev, and L. W. Molenkamp, *Phys. Rev. Lett.* **95**, 176602 (2005).
 - ²⁴ E. A. Hoffmann, H. A. Nilsson, J. E. Matthews, N. Nakpathomkun, A. I. Persson, L. Samuelson, and H. Linke, *Nano Letters* **9**, 779 (2009).
 - ²⁵ H. A. Nilsson, O. Karlström, M. Larsson, P. Caroff, J. N. Pedersen, L. Samuelson, A. Wacker, L.-E. Wernersson, and H. Q. Xu, *Phys. Rev. Lett.* **104**, 186804 (2010).
 - ²⁶ H. A. Nilsson, P. Caroff, C. Thelander, M. Larsson, J. B. Wagner, L. Wernersson, L. Samuelson, and H. Q. Xu, *Nano Letters* **9**, 3151 (2009).
 - ²⁷ P. J. Walsh, K. C. Gordon, D. L. Officer, and W. M. Campbell, *J. Mol. Struct. (THEOCHEM)* **759**, 17 (2006).
 - ²⁸ Y. Xue, S. Datta, and M. A. Ratner, *Journal of Chemical Physics* **115**, 4292 (2001).
 - ²⁹ Y. Xue, S. Datta, and M. A. Ratner, *Chemical Physics* **281**, 151 (2002).
 - ³⁰ W. Tian, S. Datta, S. Hong, R. Reifenberger, J. I. Henderson, and C. P. Kubiak, *J. Chem. Phys.* **109**, 2874 (1998).

³¹ N. Mingo, Phys. Rev. B **74**, 125402 (2006).

³² A. A. Jarzecki, P. M. Kozlowski, P. Pulay, B.-H. Ye, and X.-Y. Li, Spectrochimica Acta Part A **53**, 1195 (1997).

³³ J. N. Pedersen and A. Wacker, Phys. Rev. B **72**, 195330 (2005).